

Article

# Spin Polarization of Electrons in Two-Color XUV + Optical Photoionization of Atoms

Nikolay M. Kabachnik <sup>1,2,\*</sup>  and Irina P. Sazhina <sup>2</sup><sup>1</sup> Donostia International Physics Center, E-20018 Donostia-San Sebastian, Spain<sup>2</sup> Skobeltsyn Institute of Nuclear Physics, Lomonosov Moscow State University, 119991 Moscow, Russia; isazhina@mail.ru

\* Correspondence: nkabach@gmail.com

**Abstract:** The spin polarization of photoelectrons in two-color XUV + optical multiphoton ionization is theoretically considered using strong field approximation. We assume that both the XUV and the optical radiation are circularly polarized. It is shown that the spin polarization is basically determined by the XUV photoabsorption and that the sidebands are spin polarized as well. Their polarization may be larger or smaller than that of the central photoelectron line depending on the helicity of the dressing field.

**Keywords:** multiphoton ionization; two-color; photoelectrons; spin polarization; femtosecond pulses; xenon atom

## 1. Introduction

The spin polarization of photoelectrons is one of the fundamental characteristics of photoionization processes. Starting from the pioneering paper by U. Fano [1] and the seminal papers by M. Amusia's pupil N. Cherepkov [2,3], it was realized that in spite of the weakness of the spin-orbit interaction, the spin polarization of photoelectrons may be large, of the order of unity. During the last 50 years, a large number of experimental and theoretical works have been devoted to studying the spin polarization of photoelectrons in the photoemission from atoms, molecules and solids (see [3–5] and references therein). There are two main reasons why these investigations are considered important. One is that a high degree of polarization of photoelectrons is an important prerequisite for creating sources of polarized electrons, which in turn may serve as a tool for investigating various aspects of magnetism in solids [6,7]. Another reason is that measurements of spin polarization provide additional information about the mechanism of the photoemission; in particular, they are necessary for the realization of the so-called complete experiment, i.e., the experimental determination of the complex amplitudes of photoionization [8].

Until quite recently, the majority of the experimental investigations of spin polarization of photoelectrons have been performed at synchrotron radiation sources. Since the intensity of the sources is rather low, the interpretation of these experiments was based on the linear single-photon approximation describing the interaction of the photons with a quantum system. Spin polarization in multiphoton processes has been considered theoretically first for relatively weak laser fields where perturbation theory is applicable [9–11]. Here, it was demonstrated that the degree of polarization may be high also in the multiphoton processes. With the advent of free-electron lasers with extremely high intensities of the photon beam, the possibility arises to study experimentally the spin polarization in multiphoton ionization in a wide range of photon wavelengths. A theoretical prediction of high degree of spin polarization in multiphoton strong-field ionization was presented in Ref. [12]. Recently, first experiments of this kind were reported [13–15]. Photoelectron spin polarization, in an interesting particular case of the three-photon bichromatic ( $\omega + 2\omega$ ) ionization, was theoretically considered in papers [16,17].



**Citation:** Kabachnik, N.M.; Sazhina, I.P. Spin Polarization of Electrons in Two-Color XUV + Optical Photoionization of Atoms. *Atoms* **2022**, *10*, 66. <https://doi.org/10.3390/atoms10020066>

Academic Editors: Anatoli Kheifets, Gleb Gribakin and Vadim Ivanov

Received: 6 May 2022

Accepted: 11 June 2022

Published: 20 June 2022

**Publisher's Note:** MDPI stays neutral with regard to jurisdictional claims in published maps and institutional affiliations.



**Copyright:** © 2022 by the authors. Licensee MDPI, Basel, Switzerland. This article is an open access article distributed under the terms and conditions of the Creative Commons Attribution (CC BY) license (<https://creativecommons.org/licenses/by/4.0/>).

A special case of multiphoton processes is the photoionization of atoms and molecules by extreme ultraviolet (XUV) or soft X-ray pulses in the presence of infrared (IR) or optical radiation [18]. In the following, in order to shorten the explanations, we shall discuss the XUV+IR two-color case, although all discussed properties and conclusions are also valid for ionizing by soft X-rays and for dressing by an optical pulse (OP). If the energy of the XUV photons in these two-color experiments is sufficient to ionize the atom, a series of sidebands appear in the photoelectron spectrum at both sides of the photoline, due to the simultaneous emission or absorption of the IR photons [19]. The energy separation between the sidebands is equal to the photon energy of the IR field. This process is convenient for studying the photoinduced transitions in the continuum. The appearance of the sidebands was used for measuring the duration and the arrival time of the XUV pulses from the free-electron lasers (FELs) [20,21]. Sidebands were also used for the determination of the circular polarization of the FEL beams [22,23] by measuring the circular dichroism of the sidebands.

As far as we know, there are no investigations of the spin polarization of photoelectrons generated in two-color XUV+IR processes, although it is clear that the photoelectrons both in the central line and in the sidebands should be spin polarized, provided that the fine structure of the lines is resolved in the experiment [3]. In this paper, we report a theoretical investigation of the spin polarization in such processes. We suggest a simple theoretical model based on the description of the XUV+IR processes in the strong field approximation (SFA) [24], which was widely used in the description of multiphoton processes [25]. We analyze the spin polarization of photoelectrons induced by circularly polarized XUV photons in the presence of collinear circularly polarized IR beams. In particular, we consider the component of the spin polarization parallel to the light helicity, the so-called “polarization transfer”. This component is non-zero not only in angle-resolved measurements, but also in angle-integrated experiments [4]. We show that the spin polarization of sidebands is different from the spin polarization of the central photoline and changes with the sideband order. It strongly depends on the helicity of the IR beam.

As a particular example, we chose a short-pulse two-color photoionization of Xe atoms. The ground state of Xe contains a closed 5p electronic subshell. Upon photoionization, the lowest state of the Xe<sup>+</sup> ion is a spin-orbit doublet  $^2P_{3/2}$  and  $^2P_{1/2}$ . The spin-orbit splitting is sufficiently large at 1.3 eV, which simplifies the spin-polarization measurements in which it is necessary to resolve the fine-structure components [4]. The spin polarization of photoelectrons from the single-photon ionization of Xe is well investigated both theoretically and experimentally (see, for example, [4] and references therein). Additionally, the spin polarization of emitted electrons in single-color multiphoton ionization of Xe was investigated [13–15].

In this paper, we consider the two-color multiphoton ionization of Xe by ultrashort (femtosecond) XUV and optical pulses. In the following Section 2.1, a short description of the theoretical approach is given, which is based on the strong field approximation (SFA) [24,25]. Section 2.2 contains the parameters and details of the calculation. Section 3 presents the results of the calculations as well as a discussion including simple approximate formulas for the spin polarization of the sidebands. Finally, Section 4 gives conclusions and an outlook. In the Appendix A, we present a derivation of the approximate expressions for the related matrix elements, which is used for obtaining a simple approximate expression for the spin polarization of photoelectrons in two-color experiments.

## 2. Theory

### 2.1. Theoretical Description of Spin Polarization in Two-Color Multiphoton Ionization

Consider the photoionization of an atom by two spatially and temporally overlapping electromagnetic pulses of XUV and IR radiations. Both pulses are circularly polarized and collinear, propagating along the z-axis. To describe the interaction of these pulses with the atom, we use the strong field approximation (SFA) [24,25]. We suppose that the XUV pulse is comparatively weak so that its interaction with electrons can be considered in the first-order perturbation theory, and we use the rotating wave approximation. The

IR pulse is rather strong  $10^{11}$ – $10^{13}$  W/cm<sup>2</sup>, but not strong enough to distort the bound atomic states. For a description of the atomic wave function, we use a single-active-electron approximation. The final continuum states of the emitted electron are described by the non-relativistic Volkov wave functions [26]. Note that we ignore the influence of the magnetic field of the IR pulse on the spin orientation of the emitted electron. As it was shown in paper [27], this influence is generally rather small. In this case, the amplitude of the photoionization can be written using the time-dependent distorted wave approximation as follows (we use atomic units throughout the paper unless otherwise indicated) [28]

$$A_{\vec{k}, m_s, m_j}^- = -i \int_{-\infty}^{\infty} dt \tilde{\mathcal{E}}_X(t) \langle \psi_{\vec{k}}(\vec{r}, t) \chi_{m_s} | \hat{d} | \phi_{j, m_j}(\vec{r}) \rangle e^{i(E_b - \omega_X)t}. \quad (1)$$

Here,  $\tilde{\mathcal{E}}_X(t)$  is the envelope of the XUV pulse electric field,  $\omega_X$  is its mean frequency, and  $E_b$  is the ionization potential. The matrix element  $\langle \psi_{\vec{k}}(\vec{r}, t) \chi_{m_s} | \hat{d} | \phi_{j, m_j}(\vec{r}) \rangle$  describes a transition from the initial state of the atomic electron  $\phi_{j, m_j}(\vec{r})$  with the total angular momentum and its projection  $j, m_j$ , to the final continuum state in the IR field  $\psi_{\vec{k}}(\vec{r}, t) \chi_{m_s}$  with the momentum  $\vec{k}$  and spin state  $\chi_{m_s}$ , with  $m_s$  being the projection of the spin on the  $z$  axis, and  $\hat{d}$  being the dipole operator. Note that we ignore the spin-orbit interaction in the continuum.

For a circularly polarized XUV beam with the polarization vector  $\vec{\epsilon}_X^{\pm}$ , the dipole operator is given by

$$\hat{d}^{\pm} = (\vec{\epsilon}_X^{\pm} \vec{r}) = -\sqrt{4\pi/3} r Y_{1, \pm 1}(\hat{r}), \quad (2)$$

where plus and minus signs correspond to right- and left-circularly polarized XUV photons, respectively, and  $Y_{l, m}$  is a spherical harmonic. The wave function  $\psi_{\vec{k}}(\vec{r}, t)$  in Equation (1) describes the “dressed” photoelectron in the laser field, which is characterized by the final (asymptotic) momentum  $\vec{k}$ . Within the SFA, the wave function of the photoelectron is represented by the non-relativistic Volkov wave function [26]:

$$\psi_{\vec{k}}(\vec{r}, t) = \exp \left\{ i[\vec{k} - \vec{A}_L(t)]\vec{r} - i\Phi(\vec{k}, t) \right\}. \quad (3)$$

Here,

$$\Phi(\vec{k}, t) = -\frac{1}{2} \int_t^{\infty} dt' [\vec{k} - \vec{A}_L(t')]^2 \quad (4)$$

with  $\vec{A}_L(t)$  being the vector potential of the laser field, which we define as  $\vec{A}_L(t) = \int_t^{\infty} dt' \vec{\mathcal{E}}_L(t')$  ( $\vec{\mathcal{E}}_L(t)$  is the IR laser electric field vector). For circularly polarized IR laser light,  $\vec{\mathcal{E}}_L(t)$  is

$$\vec{\mathcal{E}}_L(t) = \frac{1}{\sqrt{2}} \tilde{\mathcal{E}}_L(t) [\hat{x} \cos \omega_L t \pm \hat{y} \sin \omega_L t], \quad (5)$$

where  $\tilde{\mathcal{E}}_L(t)$  is the envelope of the laser pulse,  $\omega_L$  is its mean frequency,  $\hat{x}(\hat{y})$  is a unit vector along the  $x$  ( $y$ ) axis, and the plus (minus) sign corresponds to the right- (left-) circularly polarized IR light.

Consider the matrix element in Equation (1) and uncouple the spin angular momentum in the initial state wave function using Clebsch–Gordan coefficients:

$$\langle \psi_{\vec{k}}(\vec{r}, t) \chi_{m_s} | \hat{d} | \phi_{j, m_j}(\vec{r}) \rangle = \langle \psi_{\vec{k}}(\vec{r}, t) \chi_{m_s} | \hat{d} | \sum_{m_0, m'_s} \left( l_0 m_0, \frac{1}{2} m'_s | j m_j \right) \phi_{l_0, m_0}(\vec{r}) \chi_{m'_s} \rangle. \quad (6)$$

Here  $\phi_{\ell_0, m_0}(\vec{r})$  describes the initial state of the electron with the orbital angular momentum  $\ell_0$  and its projection  $m_0$ . Taking into account that the dipole operator does not act on the spin variables, the matrix element is reduced to

$$\langle \psi_{\vec{k}}(\vec{r}, t) \chi_{m_s} | \hat{d} | \phi_{j, m_j}(\vec{r}) \rangle = \langle \psi_{\vec{k}}(\vec{r}, t) | \hat{d} | \phi_{l_0, m_0}(\vec{r}) \rangle \left( l_0 m_0, \frac{1}{2} m_s | j m_j \right). \quad (7)$$

Substituting this expression into the amplitude (1), one obtains

$$A_{\vec{k},m_s,m_j} = (l_0 m_0, \frac{1}{2} m_s | j m_j) \delta_{m_0,m_j-m_s} \mathcal{M}_{\vec{k},m_0}, \tag{8}$$

where  $\delta_{m,m'}$  is the Kronecker symbol and

$$\mathcal{M}_{\vec{k},m_0} = -i \int_{-\infty}^{\infty} dt \tilde{\mathcal{E}}_X(t) \langle \psi_{\vec{k}}(\vec{r},t) | \hat{d} | \phi_{l_0 m_0}(\vec{r}) \rangle e^{i(E_b - \omega_X)t}. \tag{9}$$

The probability for the photoelectron to have a certain projection  $m_s$  is proportional to the square of the amplitude (8) averaged over projections  $m_j$ :

$$W_{m_s}^j(\vec{k}) = \frac{1}{2j+1} \sum_{m_j} |(l_0 m_0, \frac{1}{2} m_s | j m_j) \delta_{m_0,m_j-m_s} \mathcal{M}_{\vec{k},m_0}|^2. \tag{10}$$

In the following, we consider the z-component of the polarization vector,  $P_z^j$  which is parallel to the photon beam direction. This is the largest component in the considered energy range [3]. Additionally, this is the only non-zero component which characterizes the angle-integrated spin polarization of the total photoelectron flux. The degree of spin polarization (z-component of the polarization vector) is usually defined as the ratio

$$P_z^j(\vec{k}) = \frac{W_{1/2}^j(\vec{k}) - W_{-1/2}^j(\vec{k})}{W_{1/2}^j(\vec{k}) + W_{-1/2}^j(\vec{k})}. \tag{11}$$

In particular, for the photoionization of p atomic shell ( $l_0 = 1$ ),  $j = 1/2$ ,  $m_j = \pm 1/2$  and  $j = 3/2$ ,  $m_j = \pm 1/2, \pm 3/2$ . Then for  $j = 1/2$  one has

$$W_{1/2}^j(\vec{k}) = \frac{1}{2} \left\{ \left| \frac{1}{\sqrt{3}} \mathcal{M}_{\vec{k},0} \right|^2 + \left| \frac{\sqrt{2}}{\sqrt{3}} \mathcal{M}_{\vec{k},-1} \right|^2 \right\}, \tag{12}$$

$$W_{-1/2}^j(\vec{k}) = \frac{1}{2} \left\{ \left| \frac{\sqrt{2}}{\sqrt{3}} \mathcal{M}_{\vec{k},1} \right|^2 + \left| \frac{1}{\sqrt{3}} \mathcal{M}_{\vec{k},0} \right|^2 \right\}. \tag{13}$$

For  $j = 3/2$ , one has

$$W_{1/2}^{3/2}(\vec{k}) = \frac{1}{4} \left\{ |\mathcal{M}_{\vec{k},1}|^2 + \left| \frac{\sqrt{2}}{\sqrt{3}} \mathcal{M}_{\vec{k},0} \right|^2 + \left| \frac{1}{\sqrt{3}} \mathcal{M}_{\vec{k},-1} \right|^2 \right\}, \tag{14}$$

$$W_{-1/2}^{3/2}(\vec{k}) = \frac{1}{4} \left\{ \left| \frac{1}{\sqrt{3}} \mathcal{M}_{\vec{k},1} \right|^2 + \left| \frac{\sqrt{2}}{\sqrt{3}} \mathcal{M}_{\vec{k},0} \right|^2 + |\mathcal{M}_{\vec{k},-1}|^2 \right\}. \tag{15}$$

Thus the spin polarization  $P_z$  for the case of  $j = 1/2$  is

$$P_z^{1/2}(\vec{k}) = \frac{|\mathcal{M}_{\vec{k},-1}|^2 - |\mathcal{M}_{\vec{k},1}|^2}{|\mathcal{M}_{\vec{k},0}|^2 + |\mathcal{M}_{\vec{k},1}|^2 + |\mathcal{M}_{\vec{k},-1}|^2}, \tag{16}$$

while for  $j = 3/2$  the polarization is

$$P_z^{3/2}(\vec{k}) = \frac{|\mathcal{M}_{\vec{k},1}|^2 - |\mathcal{M}_{\vec{k},-1}|^2}{2 |\mathcal{M}_{\vec{k},0}|^2 + |\mathcal{M}_{\vec{k},1}|^2 + |\mathcal{M}_{\vec{k},-1}|^2}. \tag{17}$$

Note that in the considered model,  $P_z^{3/2}(\vec{k}) = -\frac{1}{2} P_z^{1/2}(\vec{k})$ , as it is in the single photon ionization [4].

For calculating the amplitudes  $\mathcal{M}_{\vec{k},m_0}$  we expand the continuum wave function  $\psi_{\vec{k}}$  in partial waves and apply the dipole selection rules. Then the matrix element of the dipole

operator for circularly polarized light, Equation (2), and for a particular projection  $m_0$  can be written as

$$d_{\vec{k}_0, m_0}^{\pm} = d_{\ell_0 \pm 1, m_0 \pm 1} Y_{\ell_0 \pm 1, m_0 \pm 1}(\theta_0, \phi_0) e^{i\delta_{\ell_0 \pm 1}} + d_{\ell_0 - 1, m_0 \pm 1} Y_{\ell_0 - 1, m_0 \pm 1}(\theta_0, \phi_0) e^{i\delta_{\ell_0 - 1}}. \quad (18)$$

Here  $d_{\ell_0 \pm 1, m_0 \pm 1}$  are the partial dipole amplitudes for the transitions from the initial state  $(\ell_0, m_0)$ , and  $\delta_{\ell_0 \pm 1}$  are the photoionization phases. The angles  $(\theta_0, \phi_0)$  give the direction of electron emission from the atom before propagation in the optical laser field. These angles are connected with the detection angles  $(\theta, \phi)$  after propagation in the IR field by the relations:

$$\theta_0(t) = \arccos(k_z/k_0(t)), \quad (19)$$

$$\exp(i\phi_0(t)) = \frac{(k_x - A_{Lx}(t)) + i(k_y - A_{Ly}(t))}{(k_0^2(t) - k_z^2)^{1/2}},$$

where  $k_0^2(t) = (\vec{k} - \vec{A}_L(t))^2$ .

In the particular case of p-subshell ionization ( $\ell_0 = 1, m_0 = 0, \pm 1$ ) in the absence of the IR field, s and d partial waves contribute. Then, collecting Equations (9), (18) and (19), one can obtain for a circularly polarized XUV pulse and a circularly polarized IR pulse the following expression

$$\mathcal{M}_{\vec{k}, m_0} = -i \int_{-\infty}^{\infty} dt \tilde{\mathcal{E}}_X(t) \left[ d_{2, m_0 \pm 1} Y_{2, m_0 \pm 1}(\theta_0(t), \phi_0(t)) e^{i\delta_d} + d_{0,0} \delta_{m_0 \pm 1,0} Y_{0,0} e^{i\delta_s} \right] e^{i\Phi(\vec{k}, t)} e^{i(E_b - \omega_X)t}, \quad (20)$$

where  $\delta_{m,0}$  is a Kronecker symbol.

Suppose that the XUV pulse is right-circularly polarized (upper sign in Equation (18)), then

$$\mathcal{M}_{\vec{k}, 0} = -i \int_{-\infty}^{\infty} dt \tilde{\mathcal{E}}_X(t) d_{2,1} Y_{2,1}(\theta_0(t), \phi_0(t)) e^{i\delta_d} e^{i\Phi(\vec{k}, t)} e^{i(E_b - \omega_X)t}, \quad (21)$$

$$\mathcal{M}_{\vec{k}, 1} = -i \int_{-\infty}^{\infty} dt \tilde{\mathcal{E}}_X(t) d_{2,2} Y_{2,2}(\theta_0(t), \phi_0(t)) e^{i\delta_d} e^{i\Phi(\vec{k}, t)} e^{i(E_b - \omega_X)t}, \quad (22)$$

$$\mathcal{M}_{\vec{k}, -1} = -i \int_{-\infty}^{\infty} dt \tilde{\mathcal{E}}_X(t) \left[ d_{2,0} Y_{2,0}(\theta_0(t), \phi_0(t)) e^{i\delta_d} + d_{0,0} Y_{0,0} e^{i\delta_s} \right] e^{i\Phi(\vec{k}, t)} e^{i(E_b - \omega_X)t}. \quad (23)$$

## 2.2. Choice of Parameters and Details of Calculations

In particular calculations for Xe atoms, the matrix elements  $d_{2,2}$ ,  $d_{2,1}$  and  $d_{2,0}$  and phases  $\delta_d$  and  $\delta_s$  were calculated using the Herman–Skillman potential [29] in the non-relativistic single electron model. To test the results, we calculated the spin polarization of photoelectrons by expression (16) but for a negligibly small IR field. The results agree well with more advanced calculations by Cherepkov [3] within the time-independent RPAE.

The XUV pulse was assumed to be of a Gaussian shape:

$$\tilde{\mathcal{E}}_X(t) = \exp[-(t - t_0)^2 / (2\tau_X^2)], \quad (24)$$

where  $t_0$  determines the delay of the XUV pulse relative to the optical pulse (OP), and  $\tau_X$  determines its duration. The duration FWHM was taken to be 23 fs. The duration of the OP is 60 fs, and we suppose that the XUV pulse is at the middle of the optical pulse.

The fine structure spitting of the 5p state in Xe is 1.3 eV. Therefore, in order to avoid overlapping of the two series of sidebands from 5p<sub>3/2</sub> and 5p<sub>1/2</sub> ionization, the optical

photon energy is set equal to 3.1 eV as it was chosen in a recent experiment [15]. At this photon energy, the two combs of sidebands are clearly separated, which makes it possible to determine the spin polarization for each peak [15]. For the illustrations below, we chose the electron emission angle of  $90^\circ$ , where the number of sidebands is maximal. We also present the angle-integrated polarization.

The calculated cross section and spin polarization were convoluted with a Gaussian function which imitates the energy resolution of about 0.7 eV in a possible experiment.

In the following, we assume that the XUV pulse is right circularly polarized, while the helicity of the optical pulse is changing. Below, we present the calculated spin polarization component  $P_z^{1/2}$  for the photoionization of the Xe( $5p_{1/2}$ ) state. We remind that the spin polarization for the second component of the spin-orbit doublet Xe( $5p_{3/2}$ ) can be easily obtained multiplying the calculated results by  $-1/2$ . If in an experiment the spin-orbit doublet is not resolved, the spin polarization of the photoelectrons is negligibly small [4].

### 3. Results for Ionization of Xe and Discussion

Figure 1a shows the results of the calculations for the Xe( $5p_{1/2}$ ) ionization at the XUV photon energy of 38.4 eV (photoelectron energy without optical field is 25 eV) and emission angle of  $90^\circ$ . At this energy, the calculated photoelectron spin polarization in the absence of the optical field is  $P_z^{1/2} = 0.35$ . The dressing laser intensity is  $5 \times 10^{11}$  W/cm<sup>2</sup> and photon energy is 3.1 eV. At this intensity, there are two noticeable sidebands. We remind that the XUV pulse is right-circularly polarized. When the OP is also right-circularly polarized, the electron polarization at the sidebands becomes smaller (green solid line) than at the central line. On the contrary, for the left-circular polarization of optical beam, the spin polarization at the sideband is larger than at the central line. The polarization of the central line is increasing (decreasing) when the OP is right- (left-) circularly polarized in comparison with the case of the negligible optical field. We note that the calculated polarization is practically constant along the spectral line and changes abruptly to another value at the other line.

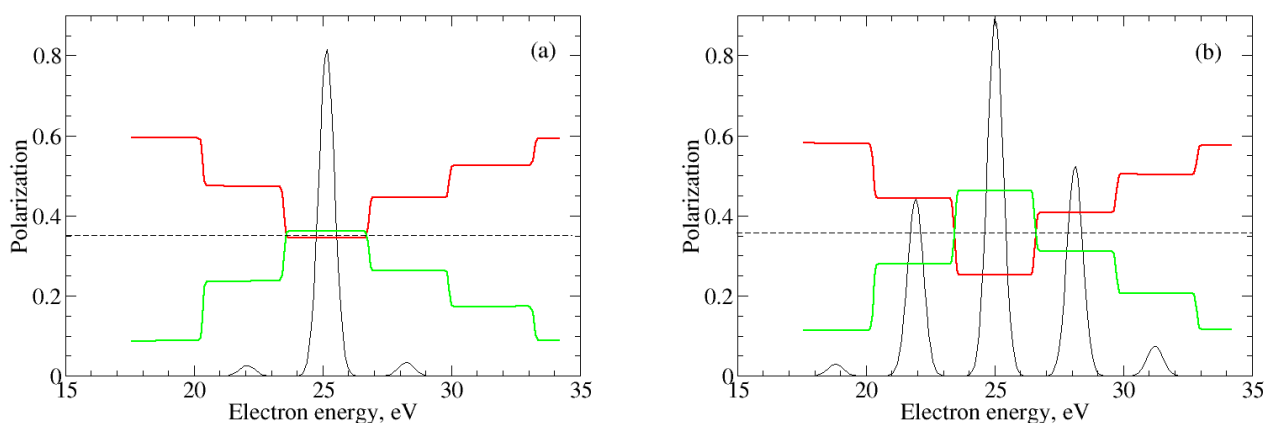


**Figure 1.** The photoelectron spin polarization component  $P_z^{1/2}$  for the XUV photon energy  $\hbar\omega_X = 38.4$  eV and the emission angle of  $90^\circ$ . Red line: left-circularly polarized dressing optical pulse (OP), green line: right-circularly polarized OP. The thin solid line shows electron spectrum in arbitrary units. The OP intensity is panel (a)  $0.5 \times 10^{12}$  W/cm<sup>2</sup>, panel (b)  $5 \times 10^{12}$  W/cm<sup>2</sup>. The dashed straight line shows the spin polarization when the OP is absent.

Figure 1b shows similar values but for larger intensity  $5 \times 10^{12}$  W/cm<sup>2</sup>. With the increase in intensity, the number of sidebands is increasing. Qualitatively, the polarization results are similar to the previous case. Note that the shift of polarization for the central line increases. From the other side, the polarization of the sidebands exhibits a weak dependence on the laser field intensity.

The angular distributions of the spin polarization for the same parameters as in Figure 1b are shown in Figure 2 (upper panel) for the central line (CL), first high-energy

sideband (SB1) and first low-energy sideband (SB-1). One can see that in all cases, the spin polarization component  $P_z^{1/2}$  has a minimum at the emission angle of  $90^\circ$ . The minimal value of polarization is different for left- and right-circularly polarized optical pulses, as it is seen also in Figure 1b. In Figure 2 (lower panel), the angular distribution of the electron yield is shown for the same parameters as in the upper panel. Interestingly, the behavior of the polarization near angles  $0^\circ$  and  $180^\circ$  is drastically different for the central line, where  $P_z^{1/2} \rightarrow 1$ , and for the first high-energy sideband at the left-polarized IR pulse and first low-energy sideband at the right-polarized IR pulse, where  $P_z^{1/2} \rightarrow 0$ .

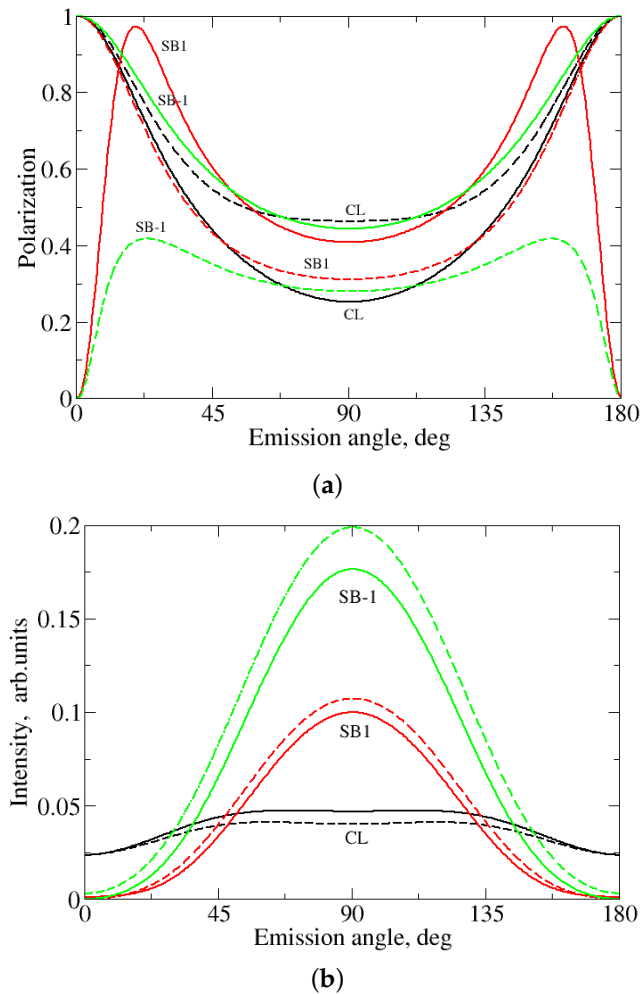
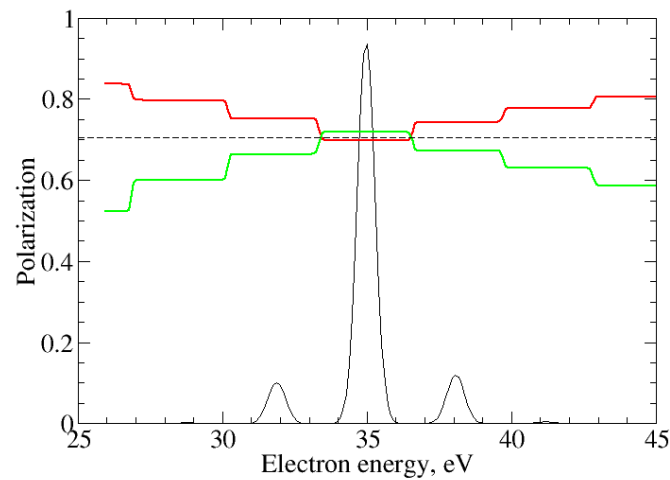


**Figure 2.** Angular distribution of the spin-polarization component  $P_z^{1/2}$  (a) and of the electron yield (b) for the XUV photon energy of 38.4 eV (the photoelectron energy without optical field is 25 eV) and the OP intensity  $5.0 \times 10^{12}$  W/cm<sup>2</sup>. Solid lines correspond to the left-circularly polarized OP, dashed lines, to the right-circularly polarized. CL denotes central line. SB1—high-energy sideband. SB-1—low-energy sideband.

This behavior may be explained using conservation of the angular momentum projection. Indeed, in our non-relativistic model, the projection of the orbital angular momentum is conserved. For the central line and right-circularly polarized XUV pulse, this gives  $M_i + m_e = +1$ , where  $M_i$  and  $m_e$  are projections of the ion and the electron orbital angular momenta. If the electron is emitted at zero angle,  $m_e = 0$  and therefore,  $M_i = 1$ . Then in the final state  $^2P_{1/2}$ , the projection of spin  $S_i$  must be  $M_s = -1/2$ . Since in photoionization the spin projection is also conserved,  $M_s + s_e = 0$  and therefore  $s_e = 1/2$ , i.e.,  $P_z^{1/2} = +1$ . For the first high-energy sideband and left-circularly polarized optical photon, the sum of the projections of XUV and laser photons is zero, and therefore  $M_i + m_e = 0$ . In the

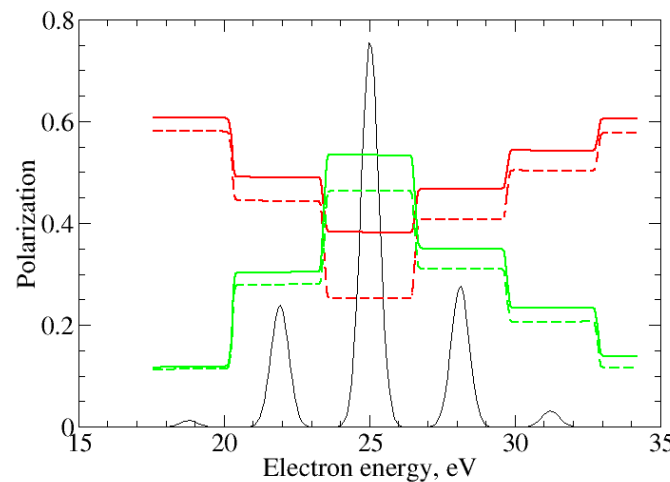
forward emission,  $m_e = 0$ , thus  $M_i = 0$  and the spin projection may be  $M_s = \pm 1/2$  with equal probability, which means that  $P_z^{1/2} = 0$ . Similarly one can show that for the first low-energy sideband and the right-circularly polarized OP photon, the polarization is also zero in the forward direction. We note that the behavior of the spin polarization in forward and backward directions, although interesting, is practically not very important since the cross section of the sideband formation at emission angles  $0^\circ$  and  $180^\circ$  is negligibly small for circularly polarized light (see lower panel of Figure 2).

Figure 3 shows the polarization for the electron energy of 35 eV and OP intensity  $1 \times 10^{12}$  W/cm<sup>2</sup>. All other parameters are the same as in Figure 1. For this energy, the electron polarization without laser field is larger [3],  $P_z^{1/2} \approx 0.7$ . When the optical radiation is switched on, the polarization for sidebands is changing similarly to the previous case.



**Figure 3.** The same as in Figure 1 but for the XUV photon energy 48.4 eV (the photoelectron energy without optical field is 35 eV) and the OP intensity is  $1.0 \times 10^{12}$  W/cm<sup>2</sup>. Red line—left-circularly polarized OP, green line—right circularly polarized OP.

The total angle-integrated polarization for sideband electrons behaves qualitatively similarly to that for the emission angle of  $90^\circ$ . As an example, the angle integrated polarization is shown in Figure 4 for the electron energy of 25 eV and laser intensity of  $5.0 \times 10^{12}$  W/cm<sup>2</sup>.



**Figure 4.** Total spin polarization  $P_z^{1/2}$  (solid lines) and spin polarization at  $90^\circ$  (dashed lines) at the XUV photon energy of 38.4 eV. Red lines: left-circularly polarized OP, green lines: right-circularly polarized OP. The IR intensity is  $5.0 \times 10^{12}$  W/cm<sup>2</sup>. The thin solid line shows the electron spectrum in arbitrary units.

The general behavior of the total (angle integrated) spin polarization is similar to that of the polarization at 90° emission angle. However, the total polarization is larger than at 90°, since the angular distribution of the polarization  $P_z^{1/2}$  has a minimum in the direction perpendicular to the beam.

Qualitatively, the above discussed behavior of the spin polarization of the photoelectrons in the dressing laser field can be explained as follows. If one assumes that both the XUV pulse and the laser pulse are sufficiently long (i.e., contain many oscillations of the electric field), then following the procedure described in paper [30], one can obtain analytical expressions for the matrix elements  $\mathcal{M}_{\vec{k},m}$ . We also make additional approximations. First, we take into account that we consider electron emission at 90°. Thus we can neglect the contribution of the matrix element  $\mathcal{M}_{\vec{k},0}$  (Equation (21)), containing the spherical function  $Y_{2,1}$  which is small around 90°. In the matrix element  $\mathcal{M}_{\vec{k},-1}$  (Equation (23)), we neglect the term containing  $d_{2,0}Y_{2,0}$ , since in the considered energy range  $d_{2,0} \ll d_{0,0}$  (i.e., the contribution of the d partial wave is much smaller than the contribution of the s partial wave). Then, using the Jacobi–Anger expansion in terms of Bessel functions, the matrix elements  $\mathcal{M}_{\vec{k},-1}$  and  $\mathcal{M}_{\vec{k},+1}$  can be presented as a sum of contributions corresponding to different sidebands (for the derivation of these expressions, see the Appendix A)

$$\mathcal{M}_{\vec{k},-1} = -i \frac{1}{\sqrt{4\pi}} d_{00} \sum_{n=-\infty}^{+\infty} \tilde{\mathcal{E}}_X^{(n)} i^n J_n(q), \tag{25}$$

$$\mathcal{M}_{\vec{k},1} = -i \frac{\sqrt{15}}{\sqrt{32\pi}} d_{22} \sum_{n=-\infty}^{+\infty} \tilde{\mathcal{E}}_X^{(n)} i^n \left[ J_n(q) \pm \frac{2A_L}{k} J'_n(q) \right]. \tag{26}$$

Here  $J_n(q)$  and  $J'_n(q)$  are Bessel functions and their derivatives,  $q = \frac{kA_L}{\omega_L}$ , where  $A_L$  is the amplitude of the laser vector potential, and

$$\tilde{\mathcal{E}}_X^{(n)} = \int dt \mathcal{E}_X(t) \exp[i(E_b - \omega_X + k^2/2 + n\omega_L)t]. \tag{27}$$

For a long pulse, the right-hand side of the last equation is close to a delta function, which expresses the energy conservation. Each term in the sums (25) and (26) presents the contribution of the  $n$ -th sideband. If one neglects the interference between different terms and the contribution from the neighboring terms, then the squares of the matrix elements (25) and (26) for the sideband number  $n$  are

$$|\mathcal{M}_{\vec{k},-1}(n)|^2 = \frac{|d_{0,0}|^2}{4\pi} [J_n(q)]^2, \tag{28}$$

$$|\mathcal{M}_{\vec{k},1}(n)|^2 = \frac{15|d_{2,2}|^2}{32\pi} \left[ J_n(q) \pm \frac{2A_L}{k} J'_n(q) \right]^2. \tag{29}$$

Ignoring small terms of the order  $(\frac{A_L}{k})^2$ , one can write the spin polarization  $P_z^j(n)$  of the  $n$ -th sideband:

$$P_z^{1/2}(n) \approx \frac{1 - \alpha \left( 1 \pm 4 \frac{A_L}{k} \frac{J'_n(q)}{J_n(q)} \right)}{1 + \alpha \left( 1 \pm 4 \frac{A_L}{k} \frac{J'_n(q)}{J_n(q)} \right)}, \tag{30}$$

where  $\alpha = \frac{15}{8} |d_{2,2}|^2 / |d_{0,0}|^2$ . Taking into account that  $\alpha \ll 1$ , one can finally obtain the following simple approximate equation for the electron spin polarization at the  $n$ -th sideband:

$$P_z^{1/2}(n) \approx 1 - 2\alpha \left[ 1 \pm 4 \frac{A_L}{k} \frac{J'_n(q)}{J_n(q)} \right]. \tag{31}$$

Upper (lower) sign in Equation (31) corresponds to the right- (left-) circularly polarized laser pulse. (We remind that the XUV pulse is assumed to be right-circularly polarized.)

For sidebands with  $n \neq 0$ , and for small  $q$ , Equation (31) can be rewritten as

$$P_z^{1/2}(n) \approx 1 - 2\alpha \left[ 1 \pm 4 \frac{|n|\omega_L}{k^2} \right]. \tag{32}$$

It follows that for the right-circularly polarized IR pulse, the electron polarization diminishes with the increase in  $|n|$ , while for the left polarized pulse, it increases, as we see in Figures 1 and 3. Additionally, the polarization of the sidebands does not depend on the IR laser intensity.

For the central line, the situation is different. Here,  $J'_0(q)/J_0(q) = -J_1(q)/J_0(q)$  and at small  $q$

$$P_z^{1/2}(n = 0) \approx 1 - 2\alpha \left[ 1 \mp 2 \frac{A_L^2}{\omega_L} \right]. \tag{33}$$

Thus, the electron polarization in the central line is larger for pulses with the same helicity and smaller when the pulses have different helicity, and the difference of polarizations increases with the increase in laser intensity. This is clearly seen in Figures 1 and 3.

#### 4. Conclusions

We presented a theoretical analysis of the spin polarization of photoelectrons in the two-color ionization of atoms by short circularly polarized XUV + optical pulses. Based on the non-relativistic SFA model, we showed that spin polarization of the main line and the sidebands can be large. Basically, it is determined by the spin polarization induced by the XUV ionization. Spin polarization in the sidebands depends strongly on the helicity of the pulses and varies with the order of the sideband. Simple approximate expressions are suggested for the spin polarization of the main line and the sidebands. As an example, the spin polarization of the 5p photoelectrons from Xe atoms is calculated. Measurements of the spin polarization in two-color experiments could give important information about the photo processes in the continuum.

**Author Contributions:** All authors have contributed to the manuscript equally. All authors have read and agreed to the published version of the manuscript.

**Funding:** This research received no external funding

**Acknowledgments:** The authors are grateful to M. Meyer for numerous useful discussions and for critical reading the manuscript. NMK is grateful to DESY (Hamburg) for hospitality and for the financial support and to Donostia International Physics Center (DIPC) for the financial support.

**Conflicts of Interest:** The authors declare no conflict of interests.

#### Appendix A

Let derive expressions (25) and (26) for the case of a long IR pulse. Suppose that the IR pulse is circularly polarized, then the pulse electric field may be presented as

$$\mathcal{E}_L(t) = g(\alpha t) \frac{\bar{\mathcal{E}}_L}{\sqrt{2}} [\hat{x} \cos(\omega_L t) \pm \hat{y} \sin(\omega_L t)], \tag{A1}$$

where  $\bar{\mathcal{E}}_L$  is the field amplitude and upper (lower) sign corresponds to right- (left-) circularly polarized IR field. The corresponding vector potential is

$$A_L(t) = g(\alpha t) A_L [\hat{x} \sin(\omega_L t) \mp \hat{y} \cos(\omega_L t)] \tag{A2}$$

with  $A_L = -\bar{\mathcal{E}}_L / \sqrt{2}\omega_L$ . Here, and in Equation (A1), we introduced an auxiliary function  $g(x)$  which is smooth, equal to unity at small  $x$  and tends to zero limit at large  $|x|$ . It allows us to calculate the integral (4) when  $t \rightarrow \pm\infty$ , and  $\alpha \rightarrow 0$ . In the following, we assume

that  $k \gg A_L$  and ignore the quadratic term  $A_L^2$  in Equation (4). In this approximation, taking into account that  $k_x = k \sin \theta \cos \phi$  and  $k_y = k \sin \theta \sin \phi$ , the Volkov phase can be presented as

$$\Phi(\vec{k}, t) = \frac{k^2}{2}t + \frac{kA_L}{\omega_L} \sin \theta \cos(\phi \mp \omega_L t). \tag{A3}$$

Substituting this expression into Equations (22) and (23) and using the Jacobi–Anger expansion,

$$\exp(ik \cos \alpha) = \sum_{n=-\infty}^{+\infty} i^n \exp(in\alpha) J_n(\kappa), \tag{A4}$$

where  $J_n(\kappa)$  is the Bessel function, one obtains for  $\mathcal{M}(\vec{k}, -1)$

$$\begin{aligned} \mathcal{M}_{\vec{k},-1} &= -i \sum_{n=-\infty}^{+\infty} \int_{-\infty}^{\infty} dt \tilde{\mathcal{E}}_X(t) d_{00} Y_{0,0} i^n \exp(in\phi) \\ &\times \exp(\mp in\omega_L t) J_n(q) \exp\left[i\left(E_b + \frac{k^2}{2} - \omega_X\right)t\right] \\ &= -id_{00} \frac{1}{\sqrt{4\pi}} \sum_{n=-\infty}^{+\infty} i^n \exp(\mp in\phi) J_n(q) \tilde{\mathcal{E}}_X^{(n)}, \end{aligned} \tag{A5}$$

where  $q = kA_L \sin \theta / \omega_L$  and the following notation is introduced:

$$\tilde{\mathcal{E}}_X^{(n)} = \int_{-\infty}^{\infty} dt \tilde{\mathcal{E}}_X(t) \exp\left[i\left(E_b - \omega_X + \frac{k^2}{2} + n\omega_L\right)t\right]. \tag{A6}$$

Similarly for  $\mathcal{M}(\vec{k}, 1)$  one obtains

$$\begin{aligned} \mathcal{M}_{\vec{k},1} &= -i \sum_{n=-\infty}^{+\infty} \int_{-\infty}^{\infty} dt \tilde{\mathcal{E}}_X(t) d_{2,2} Y_{2,2}(\theta_0, \phi_0) i^n \exp(in\phi) \\ &\times \exp(\mp in\omega_L t) J_n(q) \exp\left[i\left(E_b + \frac{k^2}{2} - \omega_X\right)t\right]. \end{aligned} \tag{A7}$$

The spherical harmonic  $Y_{2,2}(\theta_0, \phi_0)$  can be expressed in terms of angles  $\theta, \phi$  using Equation (19) as follows:

$$\begin{aligned} Y_{2,2}(\theta_0, \phi_0) &\equiv \sqrt{\frac{15}{32\pi}} \sin^2 \theta_0 \exp(i2\phi_0) \\ &\approx \sqrt{\frac{15}{32\pi}} \left[ \sin^2 \theta \exp(2i\phi) \pm 2i \frac{A_L}{k} \sin \theta \exp(i\phi) \exp(\pm i\omega_L t) \right. \\ &\quad \left. + 2 \frac{A_L}{k} \sin^3 \theta \exp(2i\phi) \sin(\omega_L t \mp \varphi) \right]. \end{aligned} \tag{A8}$$

Here, the upper (lower) sign corresponds to the right (left) circular polarization of the IR field, and we kept only linear terms in  $A_L/k$ , which is considered to be small  $A_L/k \ll 1$ . Substituting this expression into Equation (22), one obtains the matrix element  $\mathcal{M}_{\vec{k},1}$

$$\begin{aligned} \mathcal{M}_{\vec{k},1} &= -id_{2,2} \sqrt{\frac{15}{32\pi}} \sum_{n=-\infty}^{+\infty} i^n \exp(\mp in\phi) J_n(q) \\ &\times \left[ \sin^2 \theta \exp(2i\phi) \tilde{\mathcal{E}}_X^{(n)} \pm i \frac{A_L}{k} \sin \theta (2 - \sin^2 \theta) \exp(i\phi) \tilde{\mathcal{E}}_X^{(n\pm 1)} \right. \\ &\quad \left. \pm i \frac{A_L}{k} \sin^3 \theta \exp(3i\phi) \tilde{\mathcal{E}}_X^{(n\mp 1)} \right]. \end{aligned} \tag{A9}$$

This expression can be rewritten by rearranging the terms in the sums as

$$\begin{aligned} \mathcal{M}_{\vec{k},1} = & -id_{2,2} \sqrt{\frac{15}{32\pi}} \sum_{n=-\infty}^{+\infty} \tilde{\mathcal{E}}_X^{(n)} i^n \exp[i(2 \mp n)\phi] \\ & \times \left[ \sin^2 \theta J_n(q) + \frac{A_L}{k} (2 - \sin^2 \theta) J_{n\mp 1}(q) \right. \\ & \left. - \frac{A_L}{k} \sin^3 \theta J_{n\pm 1}(q) \right]. \end{aligned} \tag{A10}$$

From Equations (A5) and (A10), by setting  $\theta = 90^\circ$  and  $\phi = 0$  and using identity  $J_{n-1}(q) - J_{n+1}(q) = 2J'_n(q)$ , one obtains equations

$$\mathcal{M}_{\vec{k},-1} = -i \frac{1}{\sqrt{4\pi}} d_{00} \sum_{n=-\infty}^{+\infty} \tilde{\mathcal{E}}_X^{(n)} i^n J_n(q), \tag{A11}$$

$$\mathcal{M}_{\vec{k},1} = -i \frac{\sqrt{15}}{\sqrt{32\pi}} d_{22} \sum_{n=-\infty}^{+\infty} \tilde{\mathcal{E}}_X^{(n)} i^n \left[ J_n(q) \pm \frac{2A_L}{k} J'_n(q) \right], \tag{A12}$$

which coincide with Equations (25) and (26).

## References

1. Fano, U. Spin orientation of photoelectrons ejected by circularly polarized light. *Phys. Rev.* **1969**, *79*, 131. [[CrossRef](#)]
2. Cherepkov, N.A. Spin polarisation of photoelectrons ejected from unpolarised atoms. *J. Phys. B At. Mol. Phys.* **1979**, *12*, 1279. [[CrossRef](#)]
3. Cherepkov, N.A. Spin polarization of atomic and molecular photoelectrons. *Adv. At. Mol. Phys.* **1983**, *19*, 395–447.
4. Heinzmann, U.; Cherepkov, N.A. Spin polarization in photoionization. In *VUV and Soft X-ray Photoionization*; Becker U., Shirley D.A., Eds.; Plenum Press: New York, NY, USA, 1996; pp. 521–559.
5. Heinzmann, U.; Dill, J.H. Spin-orbit-induced photoelectron spin polarization in angle-resolved photoemission from both atomic and condensed matter targets. *J. Phys. Condens. Matter* **2012**, *24*, 173001. [[CrossRef](#)]
6. Feder, R. *Polarized Electrons in Surface Physics*; World Scientific: Singapore, 1985.
7. Kirschner, J. *Polarized Electrons at Surfaces*; Springer: Berlin, Germany, 1985.
8. Kleinpoppen, H.; Lohmann, B.; Grum-Grzhimailo, A.N. *Perfect/Complete Scattering Experiments*, Springer Series on Atomic, Optical and Plasma Physics; Springer: Berlin/Heidelberg, Germany, 2013; Volume 75.
9. Lambropoulos, P. Spin-orbit coupling and photoelectron polarization in multiphoton ionization of atoms. *Phys. Rev. Lett.* **1973**, *30*, 413. [[CrossRef](#)]
10. Lambropoulos, P. On producing totally polarized electrons through multiphoton ionization. *J. Phys. B At. Mol. Phys.* **1974**, *7*, L33. [[CrossRef](#)]
11. Nakajima, T.; Lambropoulos, P. Electron spin-polarization in single-, two- and three-photon ionization of xenon. *Europhys. Lett.* **2002**, *57*, 25. [[CrossRef](#)]
12. Barth, I.; Smirnova, O. Spin-polarized electrons produced by strong-field ionization. *Phys. Rev. A* **2013**, *88*, 013401. [[CrossRef](#)]
13. Hartung, A.; Morales, F.; Kunitski, M.; Henrichs, K.; Laucke, A.; Richter, M.; Jahnke, T.; Kalinin, A.; Schöffler, M.; Schmidt, L.H.; et al. Electron spin polarization in strong-field ionization of xenon atoms. *Nat. Photon.* **2016**, *10*, 526. [[CrossRef](#)]
14. Liu, M.-M.; Shao, Y.; Han, M.; Ge, P.; Deng, Y.; Wu, C.H.; Gong, Q.; Liu, Y. Energy- and momentum-resolved photoelectron spin polarization in multiphoton ionization of Xe by circularly polarized fields. *Phys. Rev. Lett.* **2018**, *120*, 043201. [[CrossRef](#)]
15. Trabert, D.; Hartung, A.; Eckart, S.; Trinter, F.; Kalinin, A.; Schöffler, M.; Schmidt, L.P.H.; Jahnke, T.; Kunitski, M.; Dörner, R. Spin and Angular Momentum in Strong-Field Ionization. *Phys. Rev. Lett.* **2018**, *120*, 043202. [[CrossRef](#)]
16. Gryzlova, E.V.; Popova, M.M.; Grum-Grzhimailo, A.N. Spin polarization of photoelectrons in bichromatic extreme-ultraviolet atomic ionization. *Phys. Rev. A* **2020**, *102*, 053116. [[CrossRef](#)]
17. Popova, M.M.; Gryzlova, E.V.; Kiselev, M.D.; Grum-Grzhimailo, A.N. Symmetry violation in bichromatic ionization by a free-electron laser: Photoelectron angular distribution and spin polarization. *Symmetry* **2021**, *13*, 1015. [[CrossRef](#)]
18. Meyer, M.; Costello, J.T.; Düsterer, S.; Li, W.B.; Radcliffe, P. Two-colour experiments in the gas phase. *J. Phys. B At. Mol. Opt. Phys.* **2010**, *42*, 194006. [[CrossRef](#)]
19. Glover, T.E.; Schoenlein, R.W.; Chin, A.H.; Shank, C.V. Observation of laser assisted photoelectric effect and femtosecond high order harmonic radiation. *Phys. Rev. Lett.* **1996**, *76*, 2468. [[CrossRef](#)]
20. Meyer, M.; Cubaynes, D.; O’Keeffe, P.; Luna, H.; Yeates, P.; Kennedy, E.T.; Costello, J.T.; Orr, P.; Taïeb, R.; Maquet, A.; et al. Two-color photoionization in xuv free-electron and visible laser fields. *Phys. Rev. A* **2006**, *74*, 011401(R). [[CrossRef](#)]

21. Düsterer, S.; Radcliffe, P.; Bostedt, C.; Bozek, J.; Cavalieri, A.L.; Coffee, R.; Costello, J.T.; Cubaynes, D.; DiMauro, L.F.; Ding, Y.; et al. Femtosecond x-ray pulse length characterization at the Linac Coherent Light Source free-electron laser. *New J. Phys.* **2011**, *13*, 093024. [[CrossRef](#)]
22. Mazza, T.; Ilchen, M.; Rafipoor, A.J.; Callegari, C.; Finetti, P.; Plekan, O.; Prince, K.C.; Richter, R.; Danailov, M.B.; Demidovich, A.; et al. Determining the polarization state of an extreme ultraviolet free-electron laser beam using atomic circular dichroism. *Nat. Commun.* **2014**, *5*, 4648. [[CrossRef](#)]
23. Hartmann, G.; Lindahl, A.O.; Knie, A.; Hartmann, N.; Lutman, A.A.; MacArthur, J.P.; Shevchuk, I.; Buck, J.; Galler, A.; Glowina, J.M.; et al. Circular dichroism measurements at an x-ray free-electron laser with polarization control. *Rev. Sci. Instrum.* **2016**, *87*, 083113. [[CrossRef](#)]
24. Keldysh, L.V. Ionization in the field of a strong electromagnetic wave. *Sov. Phys. JETP* **1965**, *20*, 1307.
25. Amini, K.; Biegert, J.; Calegari, F.; Chacón, A.; Ciappina, M.F.; Dauphin, A.; Efimov, D.K.; de Morisson Faria, C.F.; Giergiel, K.; Gniewek, P. Symphony on strong field approximation. *Rep. Prog. Phys.* **2019**, *82*, 116001. [[CrossRef](#)]
26. Wolkow, D.M. Über eine Klasse von Lösungen der Diracschen Gleichung. *Z. Phys.* **1935**, *94*, 250. [[CrossRef](#)]
27. Walser, M.W.; Urbach, D.J.; Hatsagortsyan, K.Z.; Hu, S.X.; Keitel, C.H. Spin and radiation in intense laser fields. *Phys. Rev. A* **2002**, *65*, 043410. [[CrossRef](#)]
28. Kazansky, A.K.; Sazhina, I.P.; Kabachnik, N.M. Angle-resolved electron spectra in short-pulse two-color XUV+IR photoionization of atoms. *Phys. Rev. A* **2010**, *82*, 033420. [[CrossRef](#)]
29. Herman, F.; Skillman, S. *Atomic Structure Calculations*; Prentice-Hall: Englewood Cliffs, NJ, USA, 1963.
30. Kazansky, A.K.; Grigorieva, A.V.; Kabachnik, N.M. Dichroism in short-pulse two-color XUV plus IR multiphoton ionization of atoms. *Phys. Rev. A* **2012**, *85*, 053409. [[CrossRef](#)]